Effects of 5-aza-2'-deoxycytidine on DNA Methylation within Female Mouse Reproductive Tissues

Mathia Colwell
University of Minnesota College of Food, Agricultural and Natural Resource Sciences
Nicole Wanner
University of Minnesota College of Veterinary Medicine
Ramya Lekha Medida
University of Minnesota College of Food, Agricultural and Natural Resource Sciences
Chelsea Drown
University of Minnesota College of Food, Agricultural and Natural Resource Sciences
Christopher Faulk (cfaulk@umn.edu)
University of Minnesota College of Food, Agricultural and Natural Resource Sciences
Laura Mauro
University of Minnesota College of Food, Agricultural and Natural Resource Sciences

Research Article

Keywords: Decitabine, DNA Methylation, Epigenetics, Female Reproductive Tract, Rodent

Posted Date: April 18th, 2022

DOI: https://doi.org/10.21203/rs.3.rs-1547192/v1

Abstract

5-aza-2'-deoxycytidine (decitabine), is a chemotherapeutic DNA methyltransferase (DNMT) inhibitor widely used to treat myelodysplastic syndrome and acute myeloid leukemias. Decitabine's anti-neoplastic activity is thought to result from inhibition of DNMTs leading to passive demethylation of 5'methylcytosines (5mC) in rapidly dividing tissues, resulting in cell death. However, we previously reported paradoxical effects on DNA methylation by decitabine in somatic tissues. Given the potential for lasting damage to DNA methylation in reproductive tissues from even short courses of decitabine in reproductive age humans, we chose to characterize its long-term effects here. Mice were treated with two clinically relevant doses of decitabine (0.15 mg/kg, 0.35 mg/kg) for 7 weeks and DNA methylation was assessed within female reproductive tract tissues. We found methylated cytosines within the ovary to be the least sensitive to decitabine exposure at both doses, whereas the uterus and the oviduct exhibited higher 5mC dysregulation, surprisingly biased towards hypermethylation at the 0.35 mg/kg dose. We identified the sites of differential methylation; revealing specific genes and pathways involved in cell differentiation, development, communication, and cell signaling that were universally altered in all tissues. In addition to our differential methylation data, we identified dysregulated transcription and pathways using RNAseq analyses. Overall, our findings show decitabine exposure causes an epigenetic insult to DNA methylation within female reproductive tissues. Our data provides evidence that further evaluation is needed to fully establish the long-term phenotypic effects post-decitabine exposure.

Introduction

5-aza-2'-deoxycytidine (Decitabine, DAC, Dacogen) is a hypomethylating chemotherapeutic drug used to treat acute myeloid leukemia and myelodysplastic syndromes[1]. Decitabine modifies cell methylation by the inhibition DNA methyltransferases (DNMTs), resulting in hypomethylation of rapidly dividing cells such as cancer[1,2]. Most chemotherapeutics target the cell cycle and cause DNA damage, harming the integrity of oocytes and sperm of exposed individuals[3,4]. The long term effects of chemotherapy usage results in decreased reproduction potential and infertility within individuals after exposure[5–7]. Thus, gonadotoxicity induced by chemotherapeutics remains a major complication post cancer treatment; and despite clinical utility as an anti-cancer agent, the epigenetic disruption to other rapidly dividing tissues deserves further investigation.

Decitabine is highly cytotoxic and effectively decreases DNA methylation within a window of dosing[8,9]. We recently published data illustrating decitabine induces both hypo- and hypermethylation within testes, liver, hippocampus, and cortex, leading to questions of its impact on reproductive tissues[10]. In addition to decreasing global[11–13] and site specific methylation[14,1516], several studies show male reproductive tissues are sensitive to decitabine exposure. For example, exposure to decitabine causes impaired spermatogenesis, reduced testes weight, but has no major fertility effects in male mice[10,17–19]. In mouse models, maternal exposure to decitabine (dose dependent) during pregnancy causes low infant survival, limb malformation, and infertility in offspring[20,21]. Additionally, maternal exposure alters the expression of DNMTs and genes controlling endometrial changes, decreasing methylation within genes essential for implantation[22]. The transcriptional profiles and epigenetic changes induced by decitabine are characterized in female specific cancer cell lines[23–26], but little is known about the epigenetic response of the female reproductive tract after a chronic exposure.

In this study, we aimed to identify whether decitabine exposure alters DNA methylation within mouse female reproductive tissues. We used a genome-wide single-base measure, reduced representation bisulfite sequencing (RRBS), to identify differentially methylated cytosines and regions, and employed pyrosequencing to confirm site specific and global changes that are known to be responsive to DAC exposure. We also measured transcriptional changes within the ovary and uterus, finding altered gene expression in pathways associated with cellular metabolism. Our data show decitabine exposure leaves a detectable impression on the methylome and transcriptome, altering pathways and genes associated with cancer. This study is the first to highlight the effects of decitabine exposure on the responsiveness of mouse female reproductive tissues.

Methods

Animals

Female mice used in this study were obtained from an agouti viable yellow (A^{vy}) colony, maintained for over 220 generations, with 93% similarity to C57BL/6J[27]. Female wild type (a/a) mice from this strain (n = 29, 6–8 weeks of age) and C57BL6/J (n = 45, 6–8 weeks of age) from Jackson Labs were used. Mice were group housed based on strain and treatment, maintained on a 12:12 light/dark cycle and had ad libitum access to the standard lab diet Envigo 2018 (18% protein) chow and water.

Decitabine Exposure Paradigm

Pharmaceutical grade decitabine (DAC) was purchased at the University of Minnesota Boynton Health Pharmacy (Minneapolis, MN). DAC was resuspended then diluted to 0.1 mg/mL concentration in saline and stored at -80°C. DAC was thawed on ice before administering. Following a previous reported exposure paradigm, mice were administered doses of 0.0 mg/kg, 0.15 mg/kg, or 0.35 mg/kg, three times a week by intraperitoneal (i.p.) injection for 7 weeks[10,18]. After 7 weeks of exposure, mice underwent a 48 hour wash out period prior to euthanasia. All somatic tissues were snap frozen and stored at -80°C until further processing.

Dosing at 0.15 mg/kg was equivalent to ~ 50% of typical human dose, while the higher 0.35 mg/kg dose was equivalent to ~ 100% of human doses recommended for acute myeloid leukemia[28]. Direct unit conversion is not possible due to surface area dosing in humans vs. body weight in mice, therefore we used ideal body weight and average height for US adult females. These doses were previously shown to cause no loss of body weight in mice[10].

DNA Isolation and Pyrosequencing

Total genomic DNA (gDNA) from snap frozen tissues were isolated from each animal using the DNeasy Blood and Tissue Kit following the manufacturer's protocol (Qiagen, Hilden, Germany). DNA yield was determined by using a NanoPhotomer N50 system. After isolation, gDNA was bisulfite converted using the EZ DNA methylation-lightning kit (Zymo Research, Irvine, CA). To detect methylated cytosines gDNA was treated with sodium bisulfite and then sequenced. Briefly, bisulfite treatment converts unmethylated cytosines to uracil by deamination, and are read as thymidine by polymerases during sequencing.

All primers were designed using Qiagen Pyromark Assay Design software version 2.0. Each primer set was designed to contain a biotinylated reverse primer and forward primer flanking the sequence of interest. PCR amplification of bisulfite converted gDNA was performed in a 30 µl solution using HotStarTaq master mix (Qiagen), forward primer and reverse primer. Amplicons were analyzed and confirmed using automated capillary electrophoresis on the Qiaxcel Advanced System (Qiagen). Amplicons were pyrosequenced on a PyroMark ID 96 instrument (Qiagen). All plates included a 0% and 100% methylated bisulfite converted control along with a no DNA template control.

RNA Seq

Total RNA was extracted from snap frozen tissues using RNeasy plus Mini Kit following the manufacturer's protocol (Qiagen). RNA was quantified using a NanoPhotomer N50 system and quality tested using the QIAxcel Advanced Instrument to confirm a RIN score > 7 before sent for sequencing. RNA-sequencing (RNA-seq) was performed at the University of Minnesota Genomics Core. RNA libraries were created using an 18 dual-indexed Illumina TruSeq Prep kit (Illumina). All libraries were combined into a single pool and sequenced across 2 lanes of a HiSeq 2500 HO 2x50-bp run. This generated > 220 M reads for each lane. All expected barcodes were detected and well represented, with mean quality scores of > Q30.

Linux command line tools and RStudio open source software (version 4.1.2) were used for RNA-seq analysis based on an RNA-seq consensus pipeline recently published by the National Aeuronautics and Space Administration (NASA) GeneLab[29]. Read quality was assessed using FastQC v0.11.7[30] and MultiQC v1.11[31] before and after read trimming. Low quality bases and adapter sequences were removed using TrimGalore! (version 0.6.5dev)[32]. Reads were aligned using STAR (version 2.7.1a)[33] and gene level read quantification was performed with RSEM (version 1.3.0)[34].

Pairwise differential expression analyses were performed with DESeq2 (version 1.32.0) with alpha set to 0.05 in the results and summary functions[35]Genes with a Benjamini-Hochberg adjusted p-value less than 0.05 were considered differentially expressed genes (DEGs). Mouse GRCm38.p6 annotation (GTF) and FASTA files downloaded from Ensembl[36] were used to generate references for both STAR and RSEM. The RNA-seq pipeline is outlined in Fig. 1. RNAseq fastq files were uploaded to the Sequence Read Archive (SRA) under BioProject: PRJNA807375.

RRBS Sequencing Methods

RRBS libraries were sequenced generating 50 bp single reads on an Illumina HiSeq 3000/4000 instrument. The sequenced reads were controlled for quality of sequencing with the FastQC tool[30].Adapter removal was performed using Trim Galore! version 0.4[32]. The cleaned reads were then aligned to the reference genome using Bismark v0.20.0[37]. Bismark is a specialized tool for mapping bisulfite-treated reads such as the ones generated in RRBS-seq experiments. Bismark requires that the reference genome first undergoes an in-silico bisulfite conversion while transforming the genome into forward (C -> T) and reverse strand (G -> A) versions. The reads producing a unique best hit to one of the bisulfite genomes were then com- pared to the unconverted genome to identify cytosine contexts (CpG, CHG or CHH - where H is A, C or T). The cytosine2coverage and bismark_methylation_extractor modules of Bismark were used to infer the methylation state of all cytosines (for every single uniquely mappable read) and their context, and to compute the percentage methylation. The reported cytosines were filtered to get only the CpGs covered in each sample. The spike-in control sequences were used at this step to check the bisulfite conversion rates and to validate the efficiency of the bisulfite treatment.

RRBS Data Analysis

Linux command line tools and Rstudio open source software (version 3.6.1) tools were used for RRBS analysis. FastQC (version 11.3) was used to assess the overall quality of the sequenced samples, and TrimGalore[32] (version 4.5) was used to trim low-quality bases (quality score lower than 20), adapter sequence (required an overlap of 6bps), and end-repair bases from the 3' end of reads. Bismark[37] (version 19.0) was used for alignment and methylation calling. Reads were aligned to the mouse reference genome (mm10) using Bowtie2[38] (version 2.3.4) with default parameter settings. Methylation calls were reported for all nucleotides with a read depth of at least 5. All paired raw fasq.gz reads from RRBS were uploaded to the Sequence Read Archive (SRA) under BioProject: PRJNA807375. The DSS R package (version 2.32.0) determined differential methylation for Ovary, Uterus, and Oviduct at doses 0.15 mg/kg and 0.35 mg/kg against the 0.0 mg/kg control treatment group[39]. To identify differentially methylated CpGs, we used the DML test function. To identify the differentially methylated regions (DMRs), we used the callDMR test function in DSS. For all tissues, our p-value threshold was set to 0.01. The annotate the DMCs and DMRs, we used the annotatr R package using the mm10 genome[40]. The function annotate_regions was used to annotate the abundance of differentially methylated regions within CpG and Genic regions. The plot_annotation and plot_categorical functions were used to generate figures in annotatr. Annotated DMCs were categorized by top DML containing genes. Each file of DMC-containing genes were enriched using ToppFun. Gene Ontology (GO) categories consisting of molecular function, biological process, cellular component, gene family, and drug were generated to include p-value and q-value. The bioinformatics pipeline for RRBS is outlined in Fig. 1.

Results

Body Weight

Mice treated with 0.35 mg/kg had decreased body weight (p-value < 0.05) compared to control, despite a gradual gain in weight over the 7-week exposure period as seen in Fig. 2. Mice treated with 0.15 mg/kg had no significant changes in body weight.

Differentially Methylated Cytosines in Ovary, Oviduct, and Uterus

To identify differential DNA methylation between tissues and DAC treatment, we analyzed ovary, oviduct, and uterus methylation by RRBS (Table 1). In the 0.15 mg/kg treatment, we found a total of 17,467 differentially methylated cytosines (DMCs) in the ovary, 20,280 DMCs in the oviduct, and 24,301 DMCs in the uterus of the 0.15 mg/kg DAC treatments (Table 1). In ovary tissue, more DMCs were hypomethylated (53%, *n* = 9,213) than hypermethylated (47%, *n* = 8,254) in the 0.15mg/kg DAC treatment. Ovary methylation was skewed towards hypomethylation (53% hypomethylated, *n* = 9,213), whereas oviduct (51% hypermethylated, DMCs: *n* = 10,349; 49% hypomethylated DMCs, *n* = 9,931) and uterus (51% hypermethylated DMCs, *n* = 12,309; 49% hypomethylated DMCs, *n* = 11,992) 0.15 mg/kg DAC treatments skewed differential methylation towards a hypermethylated status. At the 0.35 mg/kg treatment, we identified 18,699 DMCS in ovary, 19,888 DMCs in oviduct, and 26,522 DMCs in uterus. DMCs in ovary and uterus were prominently hypermethylated (65% ovary hypermethylated DMCs *n* = 12,166; 35% ovary hypomethylated DMCs, *n* = 6,533; 63% uterus hypermethylated DMCs, *n* = 16,668; 37% uterus hypomethylated DMCs, *n* = 9,854). Oviduct DMCs were preferentially hypermethylated, but the shift towards hypermethylation was not as major compared to ovary and uterus (56% hypermethylated DMCs, *n* = 11,041; 44% hypomethylated DMCs, *n* = 8,847).

Table 1
Differential Methylation Across Decitabine Dose and Tissue Identified from RRBS Data

Differentially Methylated CpGs (DMCs)						
5mC	**Ovary**		**Oviduct**		**Uterus**	
Hypermethylated Hypomethylated	*0.15 mg/kg*	*0.35 mg/kg*	*0.15 mg/kg*	*0.35 mg/kg*	*0.15 mg/kg*	*0.35 mg/kg*
	8,254 *47%* 9,213 *53%*	12,166 65% 6,533 35%	10,349 51% 9,931 49%	11,041 56% 8,847 44%	12,309 51% 11,992 49%	16,668 63% 9,854 37%
Total	*17,467*	*18,699*	*20,280*	*19,888*	*24,301*	*26,522*
Differentially Methylated Regions (DMRs)						
5mC	**Ovary**		**Oviduct**		**Uterus**	
Hypermethylated Hypomethylated	*0.15 mg/kg*	*0.35 mg/kg*	*0.15 mg/kg*	*0.35 mg/kg*	*0.15 mg/kg*	*0.35 mg/kg*
	14 48% 15 52%	18 49% 19 51%	25 51% 24 49%	29 59% 20 41%	41 56% 32 44%	45 56% 35 44%
Total	*29*	*37*	*49*	*49*	*73*	*80*

Ovary, oviduct, and uterus tissues at doses 0.15 and 0.35 mg/kg were compared to control for assessment of differential DNA methylation by decitabine exposure using RRBS data. Differential methylation was identified by using the DSS R package.

Differentially Methylated Regions in Ovary, Oviduct, and Uterus

Based on our DMCs from our RRBS analysis, we then identified unique differentially methylated regions (DMRs) based on tissue and exposure group (Table 1). We found a total of 29 DMRs in the ovary, 49 DMRs within the oviduct, and 73 DMRs within the uterus of the 0.15 mg/kg DAC treated mice. Within the 0.35 mg/kg treated group, we identified 37 DMRs within the ovary, 49 DMRs within the oviduct, and 80 DMRs within the uterus. DMRs are preferentially hypermethylated within oviduct (51%, *n* = 25 at 0.15 mg/kg; 59%, *n* = 29 at 0.35 mg/kg) and uterus (56%, *n* = 41 at 0.15 mg/kg; 56%, *n* = 45 at 0.35 mg/kg) at both doses. However, ovary (52%, *n* = 15 at 0.15 mg/kg; 51%, *n* = 19 at 0.35 mg/kg) DMRs were hypomethylated at 0.15 mg/kg and 0.35 mg/kg with lower DMRs compared to that of oviduct and uterus.

Table 2
Overlap Summary of DMCs and DMRs

DMCs		**DMRs**	
One Tissue and Dose		One Tissue and Dose	
Tissue and Dose	*Intersect*	*Tissue and Dose*	*Intersect*
Ovary 0.15 vs 0.35	5038	Ovary 0.15 vs 0.35	3
Oviduct 0.15 vs 0.35	3547	Oviduct 0.15 vs 0.35	1
Uterus 0.15 vs 0.35	3884	Uterus 0.15 vs 0.35	3
Other Tissues and Dose		Other Tissues and Dose	
Compare Tissue and Dose	*Intersect*	*Compare Tissue and Dose*	*Intersect*
Ovary vs Oviduct 0.15	621	Ovary vs Oviduct 0.15	0
Ovary vs Uterus 0.15	726	Ovary vs Uterus 0.15	0
Oviduct vs Uterus 0.15	928	Oviduct vs Uterus 0.15	0
Ovary vs Oviduct 0.35	710	Ovary vs Oviduct 0.35	0
Ovary vs Uterus 0.35	789	Ovary vs Uterus 0.35	0
Oviduct vs Uterus 0.35	966	Oviduct vs Uterus 0.35	0

Dose and tissue overlap were identified in ovary, oviduct, and uterus samples at doses 0.15 and 0.35 mg/kg using Linux (UNIX).

Intersect of DMCs and DMRs by Tissue and Dose

In order to understand whether specific genomic sites or regions tended to be repeatedly affected by DAC across tissue, we compared DMCs and DMRs by tissue and dose as shown in Table 2. In all cases, intra-tissue comparisons between doses showed greater conservation of DMCs than inter-tissue comparisons. Ovary 0.15 mg/kg and 0.35 mg/kg had the greatest DMC overlap ($n = 5038$) compared to oviduct ($n = 3547$) and uterus ($n = 3884$) at the two doses. Within tissue DMR overlap between doses had a smaller intersect within ovary ($n = 3$), oviduct ($n = 1$), and uterus ($n = 3$).

When comparing across tissues and dose intersects, uterus 0.15 mg/kg had greater overlap with oviduct ($n = 928$) and ovary ($n = 726$) compared to ovary vs. oviduct at 0.15 mg/kg ($n = 621$). Similar comparisons were seen within the 0.35 mg/kg uterus vs. oviduct ($n = 966$) and ovary ($n = 789$). Ovary and oviduct at dose 0.35 mg/kg had lower overlap ($n = 710$) compared to uterus at 0.35 mg/kg. Between tissues, no intersects were identified when comparing across tissues and dose for DMRs.

Table 3
Top Ten DMC Containing Genes

Top Ten DMC Containing Genes: RRBS											
Ovary 0.15 mg/kg						**Ovary 0.35 mg/kg**					
Gene Name	*Number of DMCs*	*Mean Differential Methylation*	*SD*	*Min. Differential Methylation*	*Max. Differnetial Methylatoin*	*Gene Name*	*Number of DMCs*	*Mean Differential Methylation*	*SD*	*Min. Differential Methylation*	*Max. Differnetial Methylatoin*
Camta1	20	9.46	60.27	-78.17	79.25	Gse1	25.00	-34.48	42.54	-82.00	63.38
Gse1	18	-31.90	45.71	-93.29	60.95	Prdm16	24.00	-19.28	54.23	-83.18	67.41
Prdm16	18	3.13	55.45	-69.01	69.62	Wwox	24.00	-31.30	46.56	-89.66	65.15
Fbrsl1	17	-29.67	47.23	-68.69	67.63	Gnas	20.00	49.88	30.83	-75.85	78.46
Foxo6	17	-4.84	46.52	-54.12	57.33	Camta1	18.00	-14.52	55.05	-89.88	73.55
Sept9	17	-12.97	57.16	-71.12	67.75	Cdh23	18.00	-14.79	53.49	-76.48	60.10
Rbfox3	16	-14.33	49.74	-68.18	58.66	Rbfox3	18.00	-18.21	58.47	-80.83	79.40
Cdh4	15	-20.21	53.91	-69.74	73.77	Rps6ka3	17.00	39.44	51.70	-75.46	83.10
Pcdh19	15	-17.41	55.92	-72.05	59.02	Sox3	16.00	20.85	48.13	-62.07	63.99
Casz1	14	16.22	51.47	-60.68	64.04	Zfhx3	16.00	-14.27	53.50	-75.56	58.31
Oviduct 0.15 mg/kg						**Oviduct 0.35 mg/kg**					
Gene Name	*Number of DMCs*	*Mean Differential Methylation*	*SD*	*Min. Differential Methylation*	*Max. Differnetial Methylatoin*	*Gene Name*	*Number of DMCs*	*Mean Differential Methylation*	*SD*	*Min. Differential Methylation*	*Max. Differnetial Methylatoin*
Gse1	32	-24.92	49.80	-77.54	68.97	Camta1	37.00	15.98	49.75	-82.58	80.04
Zfhx3	32	34.69	41.01	-62.33	76.50	Gse1	31.00	-5.52	48.15	-62.22	61.13
Camta1	29	9.35	50.53	-61.64	62.45	Zfhx3	25.00	16.85	49.32	-65.26	70.76
Prdm16	22	-8.04	50.26	-68.03	73.82	Prdm16	23.00	-18.21	49.78	-67.10	87.45
Rbfox3	21	17.44	46.62	-75.82	66.41	Cmip	17.00	-4.62	50.83	-60.74	55.88
Cdh23	20	-32.98	45.65	-77.44	67.63	Rbfox3	17.00	-7.65	53.54	-84.54	62.17
Zfx	19	-3.44	50.39	-69.05	56.21	Slit3	17.00	-25.17	39.44	-64.79	52.53
Dact3	18	-7.64	50.37	-62.00	54.82	Casz1	16.00	-22.43	45.58	-63.70	58.50
Ksr2	17	-0.18	54.31	-69.57	78.56	Cdh13	16.00	-14.30	45.66	-59.88	47.73
Bcorl1	16	13.88	54.61	-72.18	70.84	Efnb1	16.00	6.60	52.70	-57.54	71.29
Uterus 0.15mg/kg						**Uterus 0.35mg/kg**					
Gene Name	*Number of DMCs*	*Mean Differential Methylation*	*SD*	*Min. Differential Methylation*	*Max. Differnetial Methylatoin*	*Gene Name*	*Number of DMCs*	*Mean Differential Methylation*	*SD*	*Min. Differential Methylation*	*Max. Differnetial Methylatoin*
Gse1	46	-10.28	48.21	-63.07	82.20	Camta1	50.00	-9.59	45.43	-70.09	69.30
Zfhx3	35	-22.61	44.60	-69.26	62.62	Gse1	40.00	-11.06	48.40	-76.08	77.60
Prdm16	32	4.93	53.22	-79.96	68.87	Zfhx3	28.00	-10.79	50.97	-73.16	74.60
Camta1	27	-3.66	50.30	-74.35	76.04	Nav2	27.00	-11.78	43.83	-61.21	84.05
Rbfox3	24	6.13	44.53	-66.74	59.62	Prdm16	27.00	-14.60	41.83	-62.29	68.13
Wwox	24	-9.62	47.85	-68.52	57.44	Bcor	26.00	-15.31	44.49	-71.48	55.30
Sept9	23	12.55	46.24	-61.02	66.99	Gnas	25.00	43.90	26.49	-44.37	58.83
Bcor	22	-11.16	43.00	-94.72	54.93	Igsf21	24.00	-8.03	51.30	-82.73	59.90
Zfp316	22	8.59	49.17	-63.26	61.83	Wwox	24.00	-12.03	48.18	-68.42	70.32
Cmip	21	25.21	41.19	-57.90	66.71	Sox5	20.00	-15.03	40.43	-58.40	64.11

Top 10 DMC containing genes in ovary, oviduct, and uterus at doses 0.15 and 0.35 mg/kg. Top genes are ordered in highest number of DMCs within each gene.

Top Genes with DMCs and Biological Functions

We categorized genes with the greatest density of DMCs, then assessed the mean differential methylation as shown in Table 3. Our results identify Calmodulin binding transcription activator 1 (*Camata1*), Genetic suppressor Element 1 (*Gse1*), and PR Domain Zing Finger Protein 16 (*Prdm16*) as the top three genes consistently containing DMCs across tissues and doses. Genes such as RNA Binding Protein, Fox-1 Homolog 3 (*Rbfox3*) and WW Domain-Containing Oxidoreductase (*Wwox*), contain DMCs within all tissues but differ in the presence of dose. Other top DMC containing genes include BCL6 Corepressor (*Bcor*), C-Maf Inducing Protein (*Cmip*), Septin 9 (*Sept9*), Cadherin Related 23 (*Cdh23*), and Castor Zinc Finger 1 (*Casz1*).

The top ten most significantly enriched GO terms by DMC-containing genes are referenced in Table 4. At all doses and tissue types, decitabine exposure alters biological pathways relevant to anatomical structure morphogenesis, nervous system development, cell differentiation, cell development, cellular developmental process, and regulation of signaling. Other notable terms that were significant but not consistent between tissues included animal organ development, neurogenesis, regulation of cell communication, generation of neurons, and neuron differentiation.

Table 4
Top Biological Process Gene Ontology Terms

Top Biological Pathways Affected by Decitabine: RRBS					
Ovary 0.15 mg/kg			**Ovary 0.35 mg/kg**		
Name	*p.value*	*q.value.FDR .B.H*	*Name*	*p.value*	*q.value.FDR .B.H*
anatomical structure morphogenesis	0.00E + 00	0.00E + 00	anatomical structure morphogenesis	8.15E-74	1.02E-69
nervous system development	1.52E-71	1.01E-67	nervous system development	1.52E-73	1.02E-69
cell differentiation	1.24E-66	5.46E-63	cell development	3.22E-67	1.44E-63
cell development	6.06E-66	2.00E-62	generation of neurons	3.40E-61	1.14E-57
cellular developmental process	3.28E-65	8.65E-62	neurogenesis	1.98E-59	5.31E-56
animal organ development	2.40E-60	5.27E-57	regulation of signaling	3.90E-59	8.73E-56
neurogenesis	8.36E-58	1.58E-54	regulation of cell communication	1.28E-58	2.42E-55
regulation of signaling	6.91E-57	1.14E-53	neuron differentiation	1.44E-58	2.42E-55
regulation of cell communication	9.43E-57	1.38E-53	cell differentiation	3.10E-58	4.63E-55
generation of neurons	9.04E-55	1.19E-51	cellular developmental process	6.06E-56	8.14E-53
Oviduct 0.15 mg/kg			**Oviduct 0.35 mg/kg**		
Name	*p.value*	*q.value.FDR .B.H*	*Name*	*p.value*	*q.value.FDR .B.H*
anatomical structure morphogenesis	3.70E-79	5.06E-75	nervous system development	9.00E-80	1.21E-75
nervous system development	2.49E-73	1.68E-69	anatomical structure morphogenesis	1.09E-76	7.40E-73
cell differentiation	6.60E-64	2.97E-60	cell differentiation	3.55E-67	1.61E-63
cell development	4.22E-63	1.42E-59	cell development	7.18E-67	2.43E-63
cellular developmental process	3.06E-61	8.26E-58	neurogenesis	1.81E-66	4.92E-63
neurogenesis	9.65E-59	2.17E-55	animal organ development	5.99E-66	1.35E-62
animal organ development	4.20E-58	8.10E-55	cellular developmental process	9.89E-66	1.92E-62
generation of neurons	3.50E-55	5.90E-52	generation of neurons	1.37E-63	2.32E-60
regulation of cell communication	2.56E-53	3.84E-50	neuron differentiation	1.06E-60	1.60E-57
regulation of signaling	3.31E-53	4.47E-50	regulation of signaling	4.55E-54	6.17E-51
Uterus 0.15 mg/kg			**Uterus 0.35 mg/kg**		
Name	*p.value*	*q.value.FDR .B.H*	*Name*	*p.value*	*q.value.FDR .B.H*
anatomical structure morphogenesis	0.00E + 00	0.00E + 00	anatomical structure morphogenesis	5.00E-80	7.08E-76
nervous system development	0.00E + 00	1.52E-78	nervous system development	7.02E-74	4.88E-70
cell differentiation	1.49E-68	6.79E-65	regulation of signaling	6.60E-63	3.06E-59
cell development	2.54E-67	8.71E-64	cell differentiation	8.57E-62	2.98E-58
cellular developmental process	8.44E-67	2.31E-63	regulation of cell communication	6.62E-61	1.84E-57
neurogenesis	1.12E-64	2.55E-61	cell development	8.70E-61	2.02E-57
animal organ development	2.26E-63	4.11E-60	cellular developmental process	1.14E-60	2.25E-57
generation of neurons	2.40E-63	4.11E-60	neurogenesis	3.20E-59	5.56E-56
regulation of signaling	1.34E-60	2.04E-57	animal organ development	5.83E-58	9.01E-55
neuron differentiation	9.69E-60	1.33E-56	generation of neurons	2.81E-55	3.91E-52

Top ten biological pathways altered by decitabine exposure in ovary, oviduct, and uterus at doses 0.15 and 0.35 mg/kg, organized by p-value

Distribution of Differentially Methylated Regions

We investigated if the DMRs were targeted for differential methylation or if by random across the genome. Examining DMRs in relation to CpG regions (inter CpG islands, CpG islands, CpG shelves, and CpG shores), DMRs found outside of CpG islands (inter CGI) had lower quantity of expected DMRs consistently throughout all tissues in both doses when compared to a random distribution (Fig. 3 and Fig. 4). However, DMRs found within CpG islands, shelves, and

shores had greater than expected amount of DMRs compared to a random distribution. Therefore, both doses showed a bias towards altered methylation within CpG island associated CpG sites over isolated intergenic CpG sites.

Examining DMRs in relation to genic regions (promoter, intron, exon, UTR, vs. intergenic) also revealed a non-random trend (Fig. 5 and Fig. 6**)**. DMR locations in all tissues at the 0.15 mg/kg dose have a strong bias towards 1 to 5kb regions, exons, and introns. This non-random trend was recapitulated within the tissues from the 0.35 mg/kg dose at 1 to 5kb regions, promoters, 5′ UTRs, exons, and 3′ UTRs pattern). In all cases, genic regions were heavily biased targets of decitabine dysregulation over intergenic regions.

Differentially Expressed Genes and Biological Functions from RNAseq

We next identified the regulation of differentially expressed genes (DEGs) in ovary and uterus tissues at both treatments (Table 5). We identified a total of 82 DEGs within the 0.15 mg/kg treatment, and 3,987 DEGs in the 0.35 mg/kg treatment. At both doses, we found higher percentages of upregulated genes (54%, $n = 44$ at ovary 0.15 mg/kg; 52%, $n = 2{,}061$ at ovary 0.35 mg/kg) compared to downregulated genes (46%, $n = 38$ at ovary 0.15mg/kg; 48%, $n = 1{,}926$ at ovary 0.35 mg/kg). We identified fewer DEGs in uterus when compared to ovary. We found a total of 70 DEGs in uterus at treatment 0.15 mg/kg and 11 DEGs at the 0.35 mg/kg treatment. At treatment 0.15 mg/kg, we found more upregulated genes (84%, $n = 59$) compared to down regulated genes (16%, $n = 11$). At the higher dose in uterus, we identified fewer upregulated genes (27%, $n = 3$) when compared to downregulated genes (73%, $n = 8$).

Table 5
Regulation of Differentially Expressed Genes from RNA seq data

Differentially Expressed Genes (DEGs)				
	Ovary		**Uterus**	
Upregulated	*0.15 mg/kg*	*0.35 mg/kg*	*0.15 mg/kg*	*0.35 mg/kg*
Downregulated	44 54%	2,061 52%	59 84%	3 27%
	38 46%	1,926 48%	11 16%	8 73%
Total	*82*	*3,987*	*70*	*11*
Directionality of regulation in differentially expressed gene by decitabine exposure in ovary and uterus at doses 0.15 and 0.35 mg/kg.				

We next identified the top ten DEGs in ovary and uterus tissues (Table 6). Within the ovary, the gene Cytosolic phosphoenolypyruvate carboxykinase 1 (*Pck1*) was differentially expressed at both doses. Genes Kelch Like Family Member 14 (*Klhl14)* and echinoderm microtubule associate protein-like 1(*Eml1*) were expressed within the uterus at both doses. All other DEGs within the top 10 were unique to tissue or dose. We next identified the top 10 biological functions using the total set of significant DEGs (Table 7). Top dysregulated biological processes were unique to each treatment and dose. Our data highlight DAC exposure dysregulates pathways involved with tissue development at the 0.15 mg/kg treatment in ovary, whereas the 0.35 mg/kg treatment in ovary results in catabolism pathway dysregulation. Additionally, pathways involved with immune responses were dysregulated in uterus at the 0.15 mg/kg dose. We were unable to identify top dysregulated biological processes within uterus at 0.35 mg/kg.

Table 6
Differentially Expressed Genes from RNA seq data

Top Dysregulated Genes: RNA Seq					
Ovary 0.15 mg/kg			**Ovary 0.35 mg/kg**		
Name	*fold change*	*p value*	*Name*	*fold change*	*p value*
Chrdl1	-3.14	0.00	H2ac19	-11.32	0.00
Pck1	-7.17	0.00	B430305J03Rik	-8.79	0.00
Art3	-4.16	0.01	**Pck1**	-9.16	0.00
Nnat	-2.93	0.01	Trarg1	-8.93	0.00
Asb4	-2.31	0.01	Fabp4	-9.13	0.00
Chst1	-3.55	0.01	Cfd	-9.57	0.00
Retnla	-5.78	0.02	Cidec	-9.18	0.00
Adamts5	-2.55	0.02	Adipoq	-9.45	0.00
Pdzd2	-2.25	0.04	Lep	-9.53	0.00
Cmklr1	-2.89	0.05	Gm28635	-9.25	0.00
Uterus 0.15 mg/kg			**Uterus 0.35 mg/kg**		
Name	*fold change*	*p value*	*Name*	*fold change*	*p value*
Nacad	-2.75	0.00	Sorbs1	-1.79	0.00
Klhl14	-1.96	0.00	**Eml1**	-1.53	0.00
Eml1	-1.27	0.01	**Klhl14**	-1.95	0.03
Nebl	-3.85	0.01	Adam22	-2.32	0.03
Galnt16	-2.06	0.01	Abca4	2.41	0.03
Pgr	-1.61	0.02	Gm43462	-1.69	0.04
Ryr2	-2.34	0.04	Lifr	1.07	0.04
Tcf23	-1.89	0.04	Gm26581	-6.08	0.04
Fat3	-1.84	0.05	9630050E16Rik	-2.44	0.05
Mtbp	-1.49	0.05	Cap2	-1.75	0.05

Top ten differentially expressed genes by decitabine exposure in ovary and uterus at doses 0.15 and 0.35 mg/kg, organized by p-value

Pyrosequencing of Site Specific and Global Approximation for DNA Methylation

We investigated the well-established proxy for global methylation in mice, LINE transposon metylation[41,42]. The measurement at each of 4 CpG positions is averaged over thousands of LINE copies present throughout the mouse genome. Ovary and oviduct LINE methylation within all positions and dose levels were unaltered by DAC exposure (Fig. 7). In contrast, LINE methylation in uterus at dose 0.35 mg/kg was significantly lower compared to the control dose (p-value < 0.05).

We were also interested in the methylation status of CpGs within the gene *Tcf3*, since this gene is known to be sensitive to decitabine exposure[10,18]. Accordingly, we found *Tcf3* in ovary at 0.35 mg/kg at positions 3 and 6 had significantly higher methylation compared to control (Fig. 8). In oviduct at position 3, higher methylation was present in position 4, whereas positions 3 and 5 had significantly lower methylation values compared to control. Mice exposed to 0.15 mg/kg doses had significantly lower methylation within the uterus at positions 5 and 6 (p-value < 0.05).

Table 7
Top Biological Pathways Affected by Decitabine Exposure by RNA seq

Top Biological Pathways Affected by Decitabine: RNA Seq					
Ovary 0.15 mg/kg			**Ovary 0.35 mg/kg**		
Name	p-value	q-value FDR B&H	*Name*	p-value	q-value FDR B&H
transcription from RNA polymerase II promoter in response to acidic pH	1.05E-05	1.26E-02	mRNA metabolic process	1.26E-32	1.31E-28
cardiac cell fate commitment	1.47E-05	1.26E-02	protein localization to organelle	3.91E-21	2.02E-17
striated muscle tissue development	1.90E-05	1.26E-02	RNA splicing	1.14E-20	3.93E-17
muscle tissue development	2.83E-05	1.26E-02	macromolecule catabolic process	1.58E-20	4.11E-17
female genitalia development	3.10E-05	1.26E-02	cellular macromolecule catabolic process	3.63E-20	7.53E-17
cardiac muscle tissue development	3.21E-05	1.26E-02	mRNA processing	7.62E-20	1.32E-16
cellular response to potassium ion starvation	6.27E-05	1.92E-02	intracellular protein transport	1.08E-19	1.60E-16
extracellular matrix organization	7.80E-05	1.92E-02	viral process	3.88E-19	5.03E-16
extracellular structure organization	7.92E-05	1.92E-02	chromosome organization	7.66E-19	8.83E-16
external encapsulating structure organization	8.18E-05	1.92E-02	regulation of catabolic process	1.89E-18	1.96E-15
Uterus 0.15 mg/kg			**Uterus 0.35 mg/kg**		
Name	p-value	q-value FDR B&H	*Name* p-value q-value FDR B&H		
type I interferon signaling pathway	1.57E-07	1.64E-04	NA		
cellular response to type I interferon	1.67E-07	1.64E-04			
response to type I interferon	2.26E-07	1.64E-04			
defense response to other organism	1.61E-05	7.28E-03			
response to cytokine	1.68E-05	7.28E-03			
response to virus	5.51E-05	1.50E-02			
response to other organism	7.00E-05	1.50E-02			
response to external biotic stimulus	7.09E-05	1.50E-02			
defense response	7.19E-05	1.50E-02			
defense response to virus	8.98E-05	1.50E-02			

Top biological pathways affected by decitabine exposure in ovary and uterus at doses 0.15 and 0.35 mg/kg, organized by p-value. No results were generated from Uterus 0.35 mg/kg data.

Discussion

Little is known about the lasting impact of hypomethylating chemotherapeutic exposures on the epigenome within the reproductive tract. This is the first study to explore the genome-wide effects on DNA methylation *in vivo* on the response of the female reproductive tract to a chronic, low dose decitabine exposure in mice. Our analysis identified the disruption of essential reproductive genes that also overlap with cancer related functions. This data provides

evidence that decitabine could affect normal reproductive function and therefore affect the future fertility of female patients. We discuss the following implications below.

In contrast to the proposed mechanism of decitabine, we saw equal or greater numbers of hypermethylated CpG sites across all tissues and doses. This was consistent with our previous findings on non-reproductive tissues where DMRs were preferentially hypermethylated at both doses (0.15 mg/kg and 0.35 mg/kg) in liver tissue when compared to testes[10]. Exposures within ovary at 0.35 mg/kg, oviduct at 0.15 mg/kg, and uterus at 0.35 mg/kg have the highest response of DMCs. Decitabine exposure resulted in more hypomethylated DMCs only within the ovary at dose 0.15 mg/kg. Similar results are seen with DMRs, where ovary at both doses has preferentially hypomethylated regions compared to oviduct and uterus. The abundance of hypermethylated DMCs compared to hypomethylated DMCs were unexpected based off the pharmacokinetic nature of decitabine[43]. Additional investigation is needed to unveil the mechanism behind preferential hypermethylation in reproductive and non-reproductive tissues.

Compared to other epigenetically active agents, we identified an extensive magnitude of DMCs by decitabine exposure. Here we measured an average of 17k, 20k, and 24k DMCs for each tissue at dose 0.15 mg/kg, with a slight increase of DMCs in ovary and uterus at dose 0.35 mg/kg. In contrast, a subacute exposure of cannabidiol in male mice found just ~ 3,323 DMCs in hippocampus[44]. Another study examining perinatal phthalate exposure only identified a total of 1654 DMCs in females and 1187 DMCs in males[45]. Similar detection limits of under 3000 DMCs are seen in developmental lead[46], alcohol[47], and cannabidiol[48] exposure, with even fewer detected DMRs. In contrast to these studies, we measured an average of 17k, 20k, and 24k DMCs for each tissue at dose 0.15 mg/kg, with a slight increase of DMCs in ovary and uterus at dose 0.35 mg/kg. These changes in the methylome reveal an additional layer to the complexity of potential damage to reproductive function. Further studies are needed to determine if the abundance of DMCs by decitabine exposure contribute to fertility complications or long-term damage to the reproductive system.

Our RNA seq data finds an even distribution of upregulated and downregulated genes in ovary, and bias towards upregulated genes in 0.15 m/kg uterus and downregulated genes in 0.35 mg/kg uterus. Data from our DMCs and DEGs in the uterus 0.35 mg/kg align with the hypothesis that hypermethylated DMCs are correlated with downregulated DEGs, despite the low total. In uterus 0.15 mg/kg, DMCs are evenly distributed (51% hypermethylated, 49% hypomethylated), however the DEGs are skewed towards upregulation (84% upregulated, 16% downregulated). This mismatch of DMCs and DEGs could be explained by several hypotheses. The mismatch of 0.15 mg/kg DMCs to DEGs could be a bias in position of the DMCs towards intergenic regions instead of promoters. Additionally, a higher amount of DEGs present in the 0.15 mg/kg dose compared to 0.35 mg/kg could be survivorship bias. It is unclear if our results indicate greater cell death in the 0.35 mg/kg dose, killing a subset of cell types resulting in skewed DEG results. Alternatively, the skewed DEGs may be a result of non-monotonic response between 0.15 mg/kg and 0.35 mg/kg that does not impact the DMCs, but does affect DEGs. Further investigation is needed to identify the role of mismatched DEGs to DMCs and their impact on tissue function.

We see much greater overlap of DMCs within a tissue across doses than across tissues. This agrees with previous reports of methylomes being tissue-specific and is expected. Genome methylation patterns are good predictors of tissue type and therefore alterations in the methylome are expected to occur in similar locations for a given tissue across different doses of an environmental insult[49]. Interestingly, ovary had the highest tissue intersect of DMCs across doses compared to oviduct and uterus, but had the lowest total DMCs when compared to other tissues. It is unclear if overlapping DMCs across tissues are indicative of similar function or by random change. Thus further investigation is needed to link the significance of overlapping DMCs between tissues.

Our data reflect preferential DMR distribution in open chromatin regions (OCRs). OCRs are associated with DNA regulatory elements and have a role in DNA replication, nuclear organization, and gene transcription[50]. In regards to CpGs sites, DMRs are enriched within CGIs, suggesting greater activity at OCRs over changes in methylation at isolated intergenic CpG sites. The distribution in relation to genic regions is heavily biased towards genes over intergenic regions, again suggesting higher activity of decitabine at OCRs. This finding provides further evidence of the mechanistic incorporation of decitabine and the disruption within the female reproductive tract.

While several genes we identified have roles outside of cancer pathogenesis, we identified differential methylated genes that are present, contribute to, or have a role with oncogenic properties. For example, *Camta1* expression is essential in cell proliferation and cell cycle regulation, where over expression inhibits cell growth, migration, and cell cycle in gliomas[51]. Our data reflect *Camta1* had increased DNA methylation within Ovary (0.15 mg/kg) and Oviduct (0.15 mg/kg 0.35 mg/kg), and decreased methylation in others Ovary (0.35 mg/kg) and Uterus (0.15 mg/kg, 0.35 mg/kg). A similar pattern of mismatched methylation patterning is seen in *Prdm16* and *Gse1*. *Prdm16* is a transcriptional regulator that displays histone methyltransferase activity and that plays a significant role in myelodysplastic syndrome(MDS) and acute myeloid leukemia (AML) pathologies[52]. Over expression of *Gse1* in breast cancer cells results in suppressed cancer cell proliferation, migration, and invasion[53]. In contrast, the dysregulated signaling of *Gse1-Tacstd2* drives metastatic disease, castration resistance, and disease progression[54]. Further, *Gse1* and *Cdh23*[55], a gene associated with hearing loss and breast cancer, both show high density of DMLs paired with negative differential methylation. Additionally, genes *Wwox*[56], *Bcor*[57], *Cmip*[58], and *Sept9*[59] are associated with oncogenic traits.

The top biological pathways and genes identified by our RNA sequencing transcripts did not directly correlate with our RRBS data. Our data suggests the biological pathways detected are at random and indicative of decitabine exposure causing non-targeted transcript amplification. Nevertheless, our data highlights the need to further research the impacts of chemotherapeutics on reproductive function after therapy.

It is unclear if our transcriptional data reflects the off-target effects of decitabine on proteins other than DNMTs. For example, methyl-CpG-binding domain (MBD) proteins have methylation binding domains and transcription repression domains that are dependent on methylation to determine the transcriptional state of the epigenome[60]. In a study that explored the effects of hypomethylation caused by decitabine exposure and the effects on MBD proteins in HeLa cells, MBD proteins continue to interact with downstream transcriptional regulators despite the presence of decitabine[61]. Further research is needed to determine if the interaction of decitabine with methylation dependent proteins causes dysregulated transcriptional changes.

Decitabine is not expected to have a regional bias since it is thought to randomly insert during DNA replication during cell division. If this were the case, then the genome would be expected to be globally hypomethylated. Global methylation as measured by LINE was generally unaffected, a surprising result given decitabine's purported mechanism of action, however it fits well with the genic and CpG island bias of DMRs seen in the RRBS results since LINEs are typically intergenic. Overall, decitabine appears to preferentially affect CpGs proximal to genes, which was seen in the *Tcf3* results as well. Global methylation in the high dose uterus tissue was significantly lower compared to ovary and oviduct. In contrast, CpG sites of *Tcf3* responded similar to that of testes tissue, where increased exposure results in hypomethylation of the *Tcf3* locus[10].

Our work on the impact of decitabine as a hypomethylating agent joins a growing body of evidence of chemotherapeutic literature, showing the repercussions of exposure on the female reproductive tract epigenome. This study provides one of the first surveys of the effects of decitabine on the reproductive tract methylome and include the altered biological pathways, resulting in further interrogation of female fertility and reproductive function post epigenetic chemotherapy.

Abbreviations

DNA methyltransferase (DNMT), 5'methylcytosines (5mC), genomic DNA (gDNA), differentially methylated cytosines (DMCs), reduced representation bisulfite sequencing (RRBS), differentially methylated regions (DMRs).

Declarations

AVAILABILITY

Fastq RNA-seq and RRBS reads are available in the SRA repository. (https://www.ncbi.nlm.nih.gov/sra)

ACCESSION NUMBERS

Uterus and ovary RNA-seq raw fastq reads for doses 0.0 mg/kg, 0.15 mg/kg, and 0.35 mg/kg have been deposited with the Sequence Read Archived under accession number PRJNA807375. Ovary, oviduct, and Uterus RRBS raw fastq reads for doses 0.0 mg/kg, 0.15 mg/kg, and 0.35 mg/kg have been deposited with the Sequence Read Archived submission PRJNA807375.

FUNDING

This work was supported by USDA-NIFA HATCH, AES Project. No. MIN-16-12 (CF).

ETHICS APPROVAL

All animals were maintained in accordance with the Guidelines for the Care and Use of Laboratory Animals (Institute of Laboratory Animal Resources, 1996), following the study protocol (1710-3517A) approved by the University of Minnesota Institutional Animal Care and Use Committee (IACUC).

CONSENT FOR PUBLICAITON

All authors give consent for publication of this manuscript in the Journal of Clinical Epigenetics .

CONFLICT OF INTEREST

The authors declare no conflicts of interest.

AUTHORS' CONTRIBUTIONS

Conception and design of experiments, C.F., L.M., and M.L.C, preformed experiments, M.L.C., N.W., R.L.M., C.D., data analysis, N.W. and M.L.C., interpretation and writing of the manuscript, M.L.C., N.W., C.F.

ACKNOWLEDGEMENTS

We appreciate the input from Dr. Dana Dolinoy on the topic of DNA methylation and applications of Decitabine as a hypomethylating agent.

References

1. Hackanson, B. & Daskalakis, M. Decitabine. Recent Results Cancer Res. (2014) doi:10.1007/978-3-642-54490-3_18.
2. Stresemann, C. & Lyko, F. Modes of action of the DNA methyltransferase inhibitors azacytidine and decitabine. International Journal of Cancer (2008) doi:10.1002/ijc.23607.
3. MF, M. Effect of cancer and cancer treatment on human reproduction. Expert Rev. Anticancer Ther. **7**, 811–822 (2007).
4. Delessard, M. *et al.* Molecular Sciences Exposure to Chemotherapy During Childhood or Adulthood and Consequences on Spermatogenesis and Male Fertility. doi:10.3390/ijms21041454.
5. Sonigo, C., Beau, I., Binart, N. & Grynberg, M. The Impact of Chemotherapy on the Ovaries: Molecular Aspects and the Prevention of Ovarian Damage. Int. J. Mol. Sci. **20**, (2019).

6. D, M., H, B., RA, A. & WH, W. Toxicity of chemotherapy and radiation on female reproduction. Clin. Obstet. Gynecol. **53**, 727–739 (2010).
7. CR, G. *et al.* Impact of cancer therapies on ovarian reserve. Fertil. Steril. **97**, (2012).
8. Lemaire, M. *et al.* Importance of dose-schedule of 5-aza-2'-deoxycytidine for epigenetic therapy of cancer. BMC Cancer **8**, (2008).
9. Karahoca, M. & Momparler, R. L. Pharmacokinetic and pharmacodynamic analysis of 5-aza-2'- deoxycytidine (decitabine) in the design of its dose-schedule for cancer therapy. Clinical Epigenetics vol. 5 (2013).
10. Colwell, M. *et al.* Paradoxical whole genome DNA methylation dynamics of 5'aza-deoxycytidine in chronic low-dose exposure in mice. Epigenetics **16**, (2020).
11. Yang, A. S. *et al.* DNA methylation changes after 5-aza-2'-deoxycytidine therapy in patients with leukemia. Cancer Res. (2006) doi:10.1158/0008-5472.CAN-05-2385.
12. Momparler, R. L. & Wilson, V. L. Inhibition of dna methylation in 11210 leukemic cells by 5-aza-2'-deoxycytidine as a possible mechanism of chemotherapeutic action. Cancer Res. (1983).
13. Wang, Y. *et al.* The Effects of 5-Aza-2'- Deoxycytidine and Trichostatin A on Gene Expression and DNA Methylation Status in Cloned Bovine Blastocysts. Cell. Reprogram. (2011) doi:10.1089/cell.2010.0098.
14. Ito, Y., Nativio, R. & Murrell, A. Induced DNA demethylation can reshape chromatin topology at the IGF2-H19 locus. Nucleic Acids Res. (2013) doi:10.1093/nar/gkt240.
15. Plumb, J. A., Strathdee, G., Sludden, J., Kaye, S. B. & Brown, R. Reversal of drug resistance in human tumor xenografts by 2'-deoxy-5-azacytidine-induced demethylation of the hMLH1 gene promoter. Cancer Res. (2000).
16. Negrotto, S. *et al.* CpG methylation patterns and decitabine treatment response in acute myeloid leukemia cells and normal hematopoietic precursors. Leuk. 2012 262 **26**, 244–254 (2011).
17. Kläver, R. *et al.* Direct but no transgenerational effects of decitabine and vorinostat on male fertility. PLoS One **10**, (2015).
18. Kelly, T. L. J., Li, E. & Trasler, J. M. 5-Aza-2'-Deoxycytidine Induces Alterations in Murine Spermatogenesis and Pregnancy Outcome. J. Androl. (2003) doi:10.1002/j.1939-4640.2003.tb03133.x.
19. Song, N., Endo, D., Song, B., Shibata, Y. & Koji, T. 5-aza-2'-deoxycytidine impairs mouse spermatogenesis at multiple stages through different usage of DNA methyltransferases. Toxicology (2016) doi:10.1016/j.tox.2016.07.005.
20. Vlahovi?, M. *et al.* Changes in the placenta and in the rat embryo caused by the demethylating agent 5-azacytidine. Int. J. Dev. Biol. **43**, 843–846 (2002).
21. Cisneros, F. J. & Branch, S. 5-AZA-2'-deoxycytidine (5-AZA-CdR): a demethylating agent affecting development and reproductive capacity. J. Appl. Toxicol. **23**, 115–120 (2003).
22. Ding, Y. Bin *et al.* 5-Aza-2'-deoxycytidine Leads to Reduced Embryo Implantation and Reduced Expression of DNA Methyltransferases and Essential Endometrial Genes. PLoS One **7**, (2012).
23. Logan, P. C., Ponnampalam, A. P., Rahnama, F., Lobie, P. E. & Mitchell, M. D. The effect of DNA methylation inhibitor 5-Aza-2'-deoxycytidine on human endometrial stromal cells. Hum. Reprod. **25**, 2859–2869 (2010).
24. Sova, P. *et al.* Discovery of Novel Methylation Biomarkers in Cervical Carcinoma by Global Demethylation and Microarray Analysis. Cancer Epidemiol. Prev. Biomarkers **15**, 114–123 (2006).
25. Wang, L., Tan, Y. J., Wang, M., Chen, Y. F. & Li, X. Y. DNA Methylation Inhibitor 5-Aza-2'-Deoxycytidine Modulates Endometrial Receptivity Through Upregulating HOXA10 Expression: *https://doi.org/*10.1177/*1933719118815575* **26**, 839–846 (2018).
26. Sheng, X. *et al.* Promoter hypermethylation influences the suppressive role of maternally expressed 3, a long non-coding RNA, in the development of epithelial ovarian cancer. Oncol. Rep. **32**, 277–285 (2014).
27. Weinhouse, C. *et al.* Dose-dependent incidence of hepatic tumors in adult mice following perinatal exposure to bisphenol A. Environ. Health Perspect. (2014) doi:10.1289/ehp.1307449.
28. fda & cder. HIGHLIGHTS OF PRESCRIBING INFORMATION These highlights do not include all the information needed to use DACOGEN safely and effectively. See full prescribing information for DACOGEN. DACOGEN ® (decitabine) for injection, for intravenous use.
29. Overbey, E. G. *et al.* NASA GeneLab RNA-seq consensus pipeline: Standardized processing of short-read RNA-seq data. iScience **24**, 102361 (2021).
30. Andrews, S. FASTQC A Quality Control tool for High Throughput Sequence Data. Babraham Inst. (2015).
31. Ewels, P., Magnusson, M., Lundin, S. & Käller, M. MultiQC: summarize analysis results for multiple tools and samples in a single report. Bioinformatics **32**, 3047–3048 (2016).
32. Krueger, F. Trim Galore!: A wrapper tool around Cutadapt and FastQC to consistently apply quality and adapter trimming to FastQ files. Babraham Institute (2015) doi:10.1002/maco.200603986.
33. Dobin, A. *et al.* STAR: ultrafast universal RNA-seq aligner. Bioinformatics **29**, 15–21 (2013).
34. Li, B. & Dewey, C. N. RSEM: Accurate transcript quantification from RNA-Seq data with or without a reference genome. BMC Bioinformatics **12**, 1–16 (2011).
35. Love, M. I., Huber, W. & Anders, S. Moderated estimation of fold change and dispersion for RNA-seq data with DESeq2. Genome Biol. **15**, 1–21 (2014).
36. Ensembl genome browser 104. https://useast.ensembl.org/index.html.
37. Krueger, F. & Andrews, S. R. Bismark: A flexible aligner and methylation caller for Bisulfite-Seq applications. Bioinformatics (2011) doi:10.1093/bioinformatics/btr167.

38. Langmead, B. & Salzberg, S. L. Fast gapped-read alignment with Bowtie 2. Nat. Methods (2012) doi:10.1038/nmeth.1923.
39. Park, Y. & Wu, H. Differential methylation analysis for BS-seq data under general experimental design. Bioinformatics (2016) doi:10.1093/bioinformatics/btw026.
40. Cavalcante, R. G. & Sartor, M. A. annotatr: Associating genomic regions with genomic annotations. *bioRxiv* 1–9 (2016) doi:10.1101/039685.
41. Buj, R. *et al.* Quantification of Unmethylated Alu (QUAlu): a tool to assess global hypomethylation in routine clinical samples. Oncotarget **7**, 10536–10546 (2016).
42. Yang, A. S. A simple method for estimating global DNA methylation using bisulfite PCR of repetitive DNA elements. Nucleic Acids Res. (2004) doi:10.1093/nar/gnh032.
43. Momparler, R. L. Pharmacology of 5-Aza-2'-deoxycytidine (decitabine). Semin. Hematol. (2005).
44. Wanner, N. M., Colwell, M., Drown, C. & Faulk, C. Subacute cannabidiol alters genome-wide DNA methylation in adult mouse hippocampus. Environ. Mol. Mutagen. **61**, 890–900 (2020).
45. Svoboda, L. K. *et al.* Sex-Specific Programming of Cardiac DNA Methylation by Developmental Phthalate Exposure. Epigenetics Insights **13**, (2020).
46. Wang, K. *et al.* Tissue- and Sex-Specific DNA Methylation Changes in Mice Perinatally Exposed to Lead (Pb). Front. Genet. **11**, 840 (2020).
47. Asimes, A. D. *et al.* Adolescent binge-pattern alcohol exposure alters genome-wide DNA methylation patterns in the hypothalamus of alcohol-naïve male offspring. Alcohol **60**, 179–189 (2017).
48. Wanner, N. M., Colwell, M., Drown, C. & Faulk, C. Developmental cannabidiol exposure increases anxiety and modifies genome-wide brain DNA methylation in adult female mice. Clin. Epigenetics 2021 131 **13**, 1–16 (2021).
49. Dor, Y. & Cedar, H. Principles of DNA methylation and their implications for biology and medicine. Lancet **392**, 777–786 (2018).
50. Tsompana, M. & Buck, M. J. Chromatin accessibility: a window into the genome. Epigenetics Chromatin *2014 71* **7**, 1–16 (2014).
51. Z, H. *et al.* CAMTA1, a novel antitumor gene, regulates proliferation and the cell cycle in glioma by inhibiting AKT phosphorylation. Cell. Signal. **79**, (2021).
52. FP, D. *et al.* PRDM16 (1p36) translocations define a distinct entity of myeloid malignancies with poor prognosis but may also occur in lymphoid malignancies. Br. J. Haematol. **156**, 76–88 (2012).
53. P, C. *et al.* GSE1 negative regulation by miR-489-5p promotes breast cancer cell proliferation and invasion. Biochem. Biophys. Res. Commun. **471**, 123–128 (2016).
54. OA, B. *et al.* Genetic Suppressor Element 1 (GSE1) Promotes the Oncogenic and Recurrent Phenotypes of Castration-Resistant Prostate Cancer by Targeting Tumor-Associated Calcium Signal Transducer 2 (TACSTD2). *Cancers (Basel).* **13**, (2021).
55. P, V. S., CRS, S. & R, K. M. The tip link protein Cadherin-23: From Hearing Loss to Cancer. Pharmacol. Res. **130**, 25–35 (2018).
56. Baryła, I., Styczeń-Binkowska, E. & Bednarek, A. K. Alteration of WWOX in human cancer, a clinical view: https://doi.*org/*10.1177/*1535370214561953* **240**, 305–314 (2015).
57. Astolfi, A. *et al.* BCOR involvement in cancer. doi:10.2217/epi-2018-0195.
58. M, O. & D, S. The Enigmatic Emerging Role of the C-Maf Inducing Protein in Cancer. Diagnostics (Basel, Switzerland) **11**, (2021).
59. L, S. & Y, L. SEPT9: A Specific Circulating Biomarker for Colorectal Cancer. Adv. Clin. Chem. **72**, 171–204 (2015).
60. Du, Q., Luu, P. L., Stirzaker, C. & Clark, S. J. Methyl-CpG-binding domain proteins: Readers of the epigenome. Epigenomics **7**, 1051–1073 (2015).
61. Sakamoto, Y. *et al.* Overlapping Roles of the Methylated DNA-binding Protein MBD1 and Polycomb Group Proteins in Transcriptional Repression of HOXA Genes and Heterochromatin Foci Formation. J. Biol. Chem. **282**, 16391–16400 (2007).

Figures

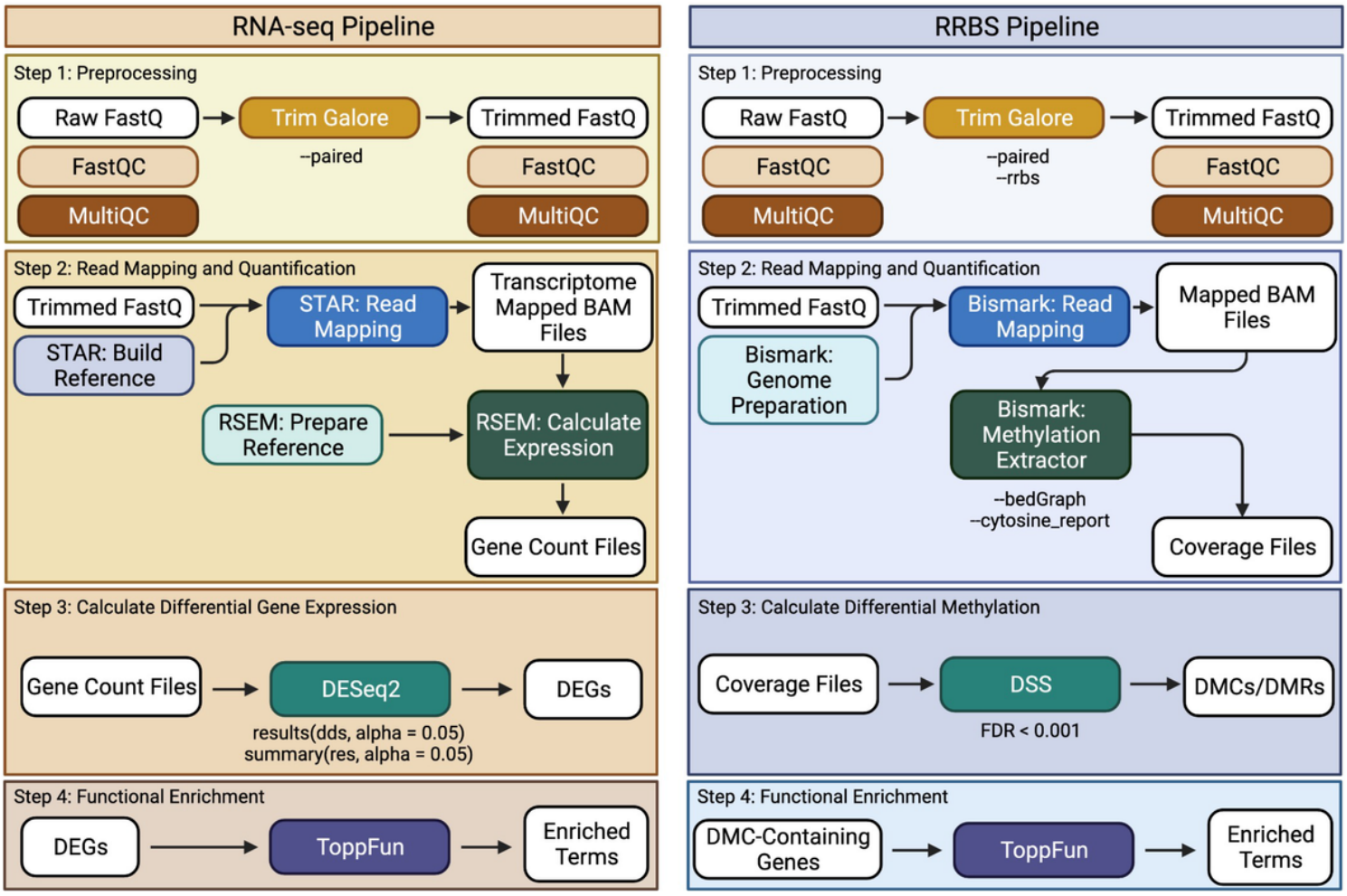

Figure 1

Bioinformatics Pipeline of Reduced Represented Bisulfite Sequencing (RRBS) and RNA-seq Pipeline RRBS and RNA-seq pipelines were processed separately. The goal of the RRBS pipeline was to identify differentially methylated CpG sites and regions within multiple female reproductive tissues, and to categorize top differentially regulated genes and pathways by decitabine exposure.

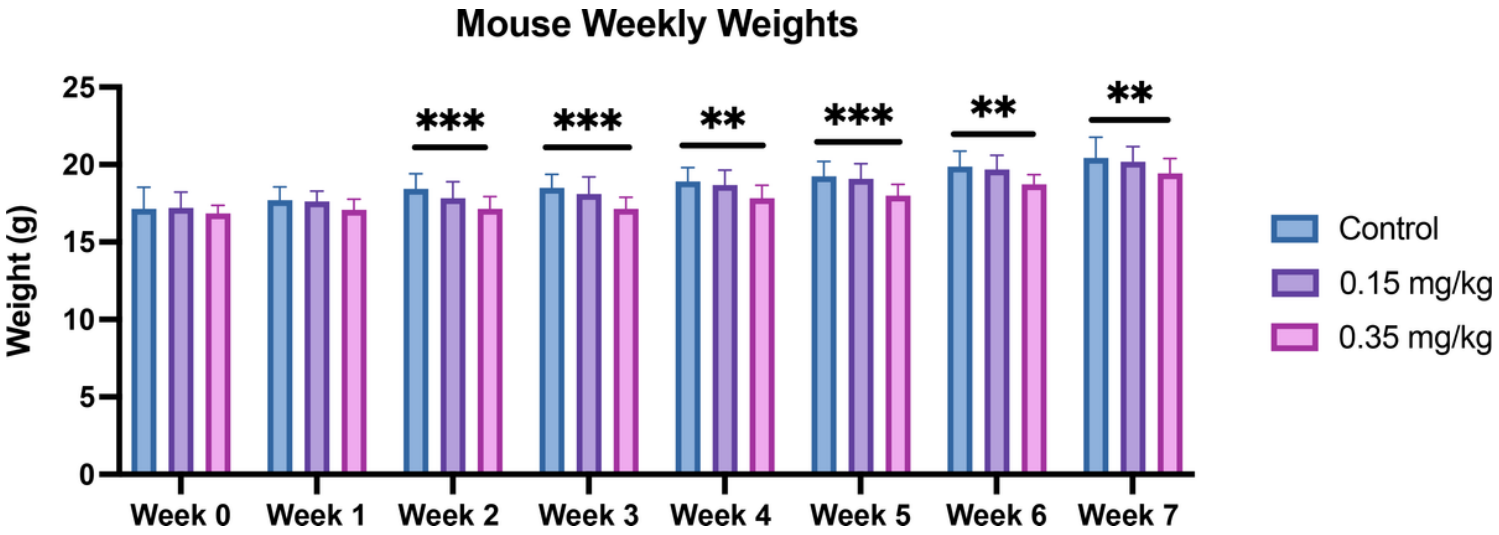

Figure 2

Mouse weights over 7 week exposure paradigm. Mice in 0.35mg/kg had significantly lower body weight starting at week 2 and persisted through week 7. (±SEM **p<0.005, **p<0.055 standard error of mean)

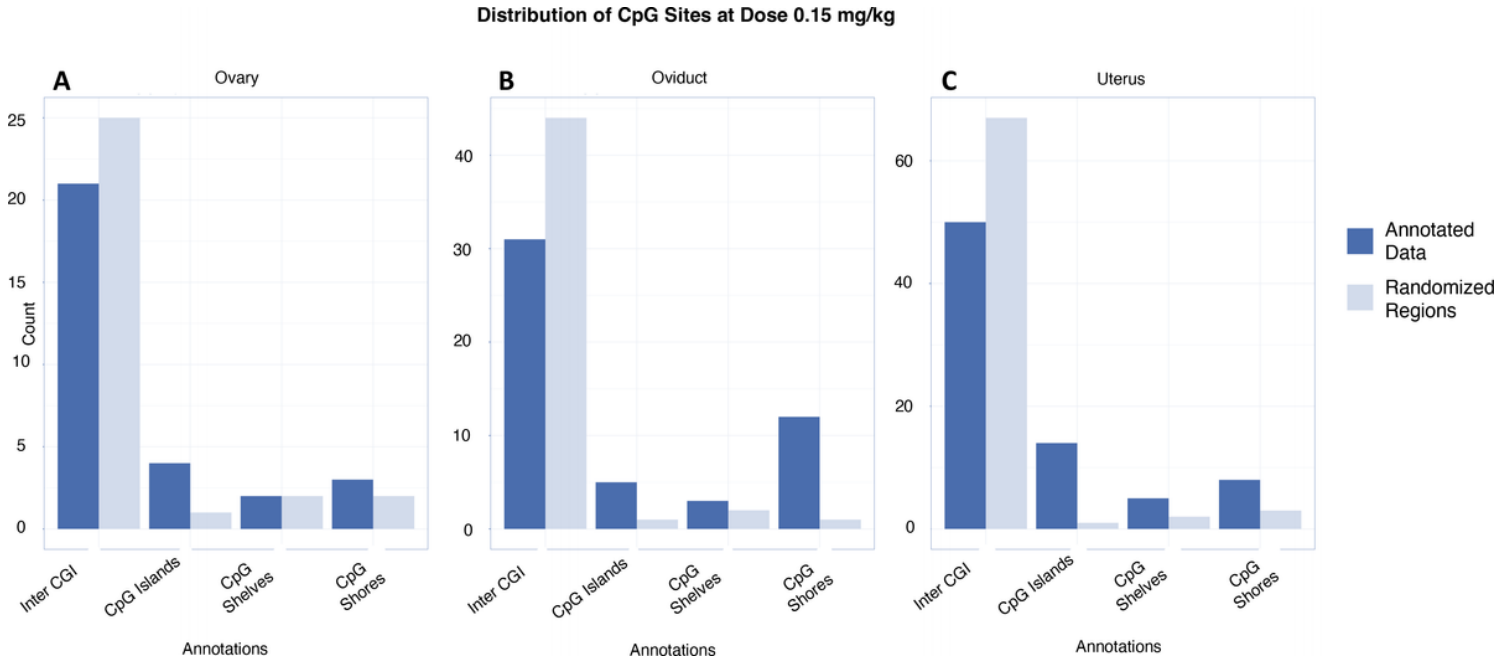

Figure 3

Annotated CpG Sites in Ovary, Oviduct, and Uterus at dose 0.15 mg/kg Distribution of CpG site DMRs within (A) Ovary (B) Oviduct and (C) Uterus at dose 0.15 mg/kg. Annotated data is plotted against a randomized set of regions.

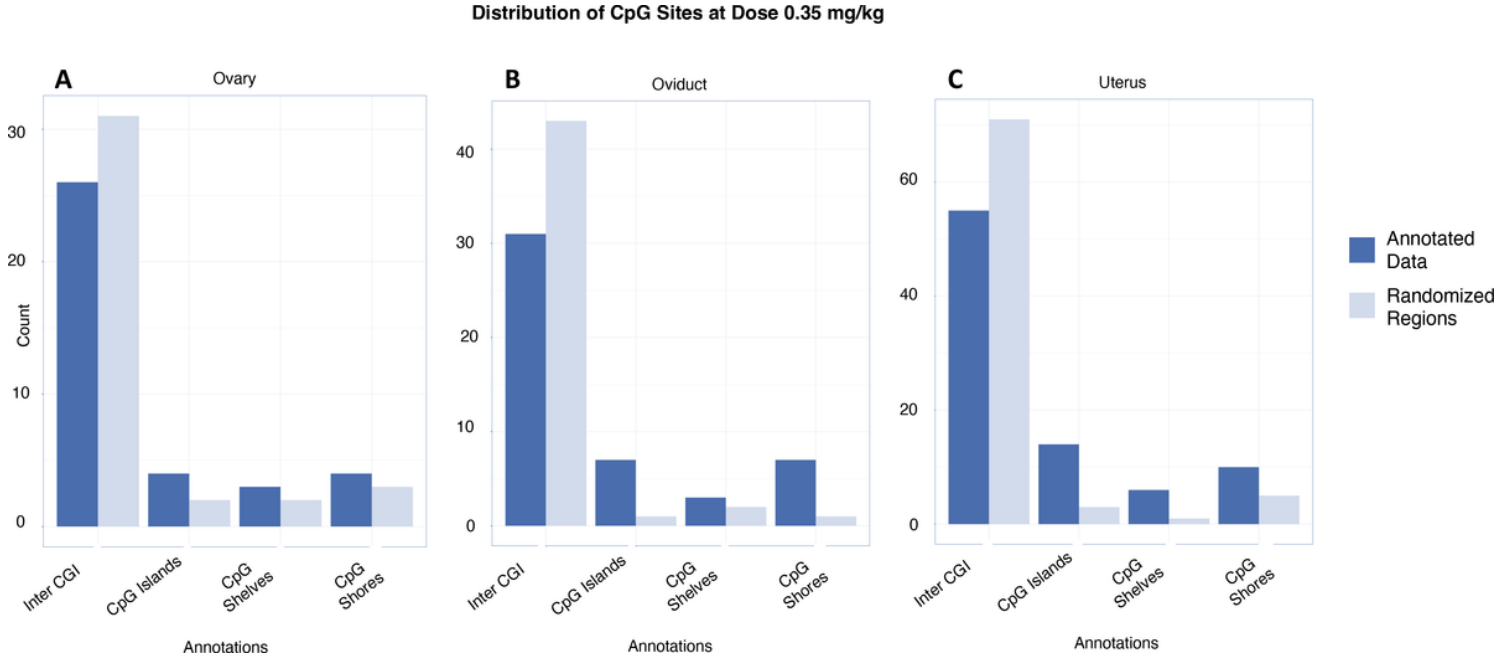

Figure 4

Annotated CpG Sites in Ovary, Oviduct, and Uterus at dose 0.35 mg/kg Distribution of CpG site DMRs within (A) Ovary (B) Oviduct and (C) Uterus at dose 0.35 mg/kg. Annotated data is plotted against a randomized set of regions.

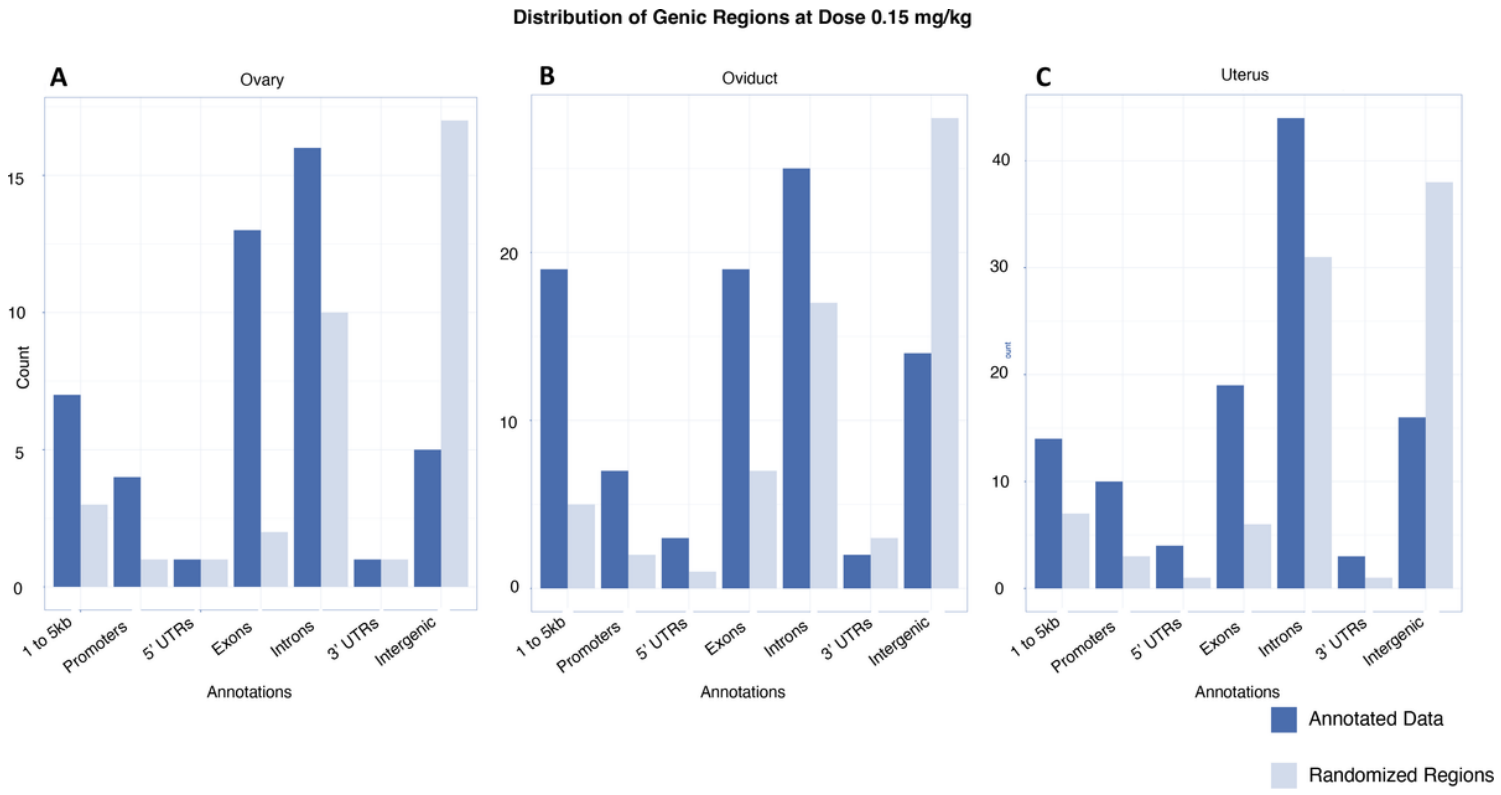

Figure 5

Annotated Genic Regions in Ovary, Oviduct, and Uterus at dose 0.15 mg/kg Distribution of genic region DMRs within (A) Ovary (B) Oviduct and (C) Uterus at dose 0.15 mg/kg. Annotated data is plotted against a randomized set of regions.

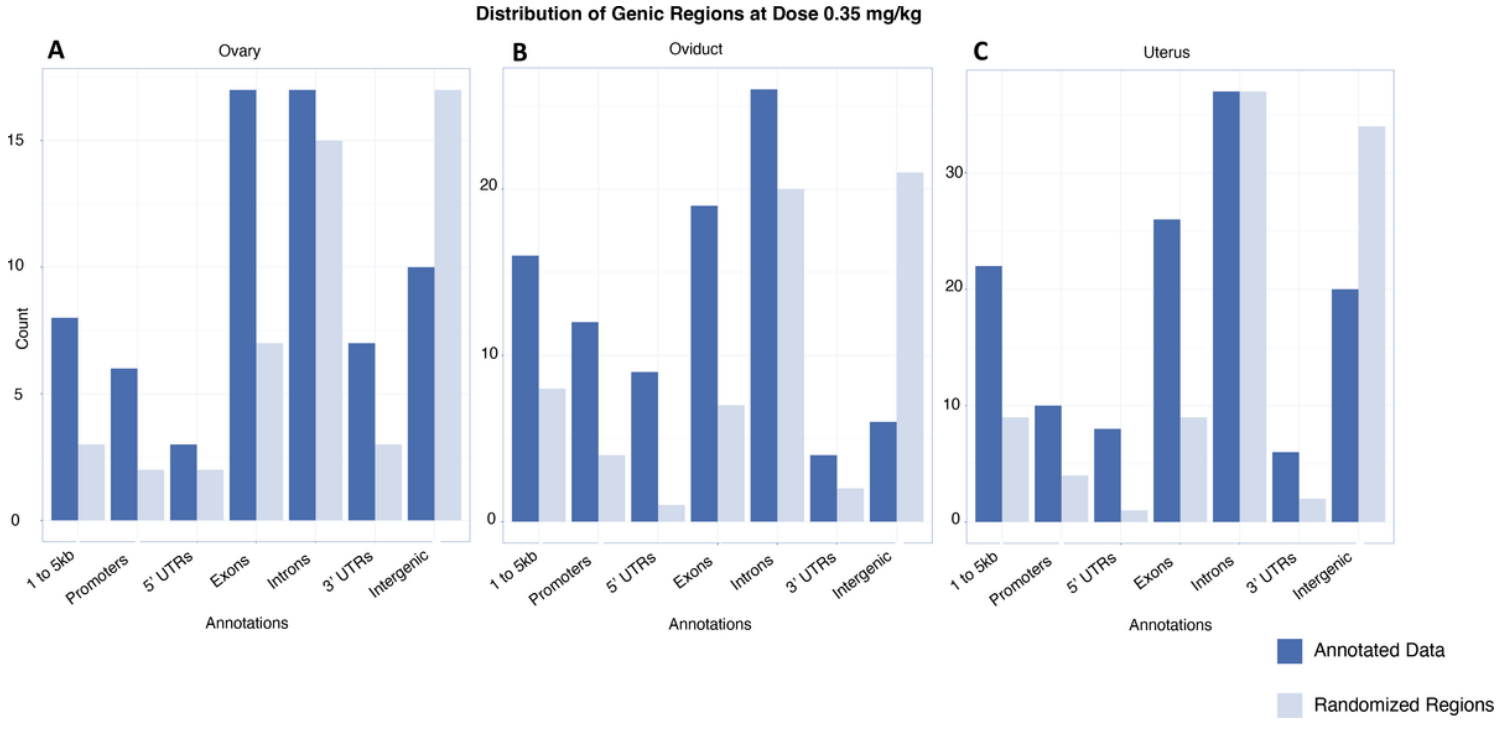

Figure 6

Annotated CpG Sites in Ovary, Oviduct, and Uterus at dose 0.35 mg/kg Distribution of DMRs within (A) Ovary (B) Oviduct and (C) Uterus at dose 0.35 mg/kg. Annotated data is plotted against a randomized set of regions.

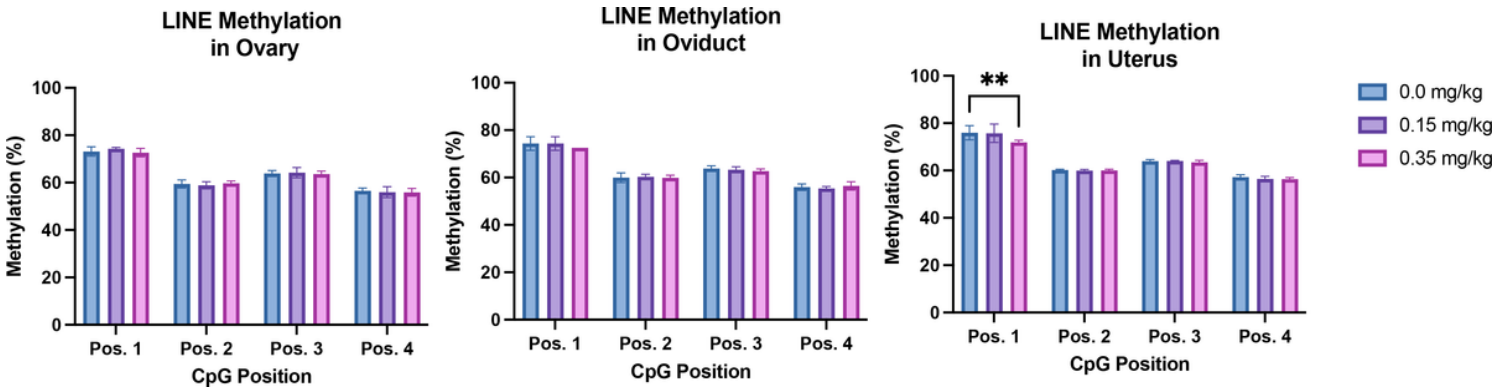

Figure 7

Mouse LINE (mLINE) methylation in Ovary, Oviduct, and Uterus Effect of DAC exposure on mLINE methylation (A) Ovary. (B) Oviduct. (C) Uterus. mLINE methylation significantly decreases at higher doses of exposure in Uterus at position one, but not at other doses or positions. Double stars indicate p-values<0.005, when compared to controls. Error bars indicate standard error.

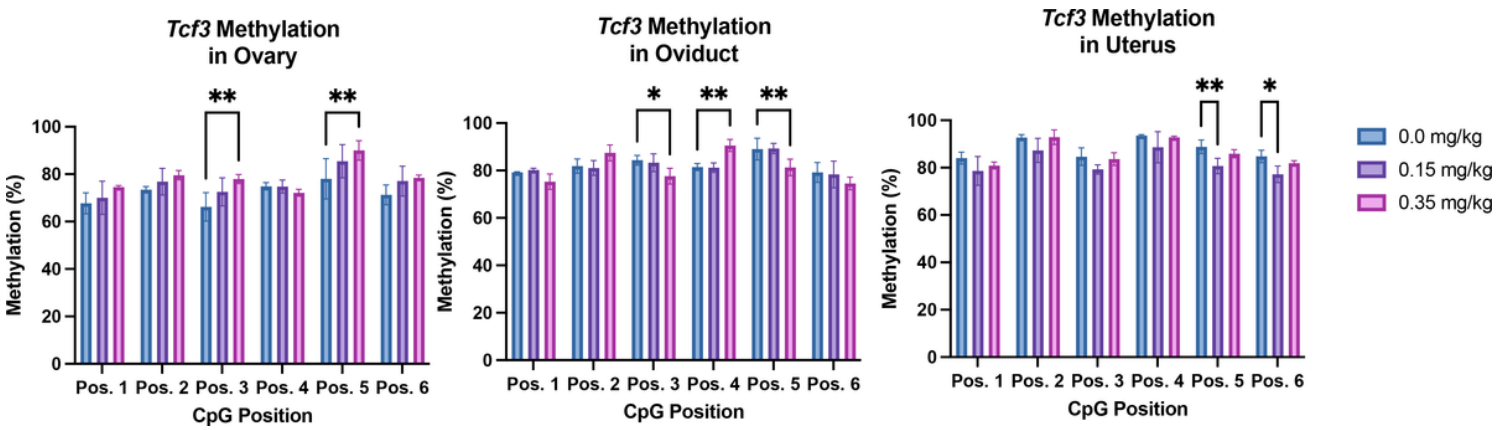

Figure 8

Tcf3 methylation in Ovary, Oviduct, and Uterus Effect of DAC exposure on *Tcf3* methylation (A) Ovary. (B) Oviduct. (C) Uterus. *Tcf3* methylation significantly increases at positions 3 and 5 in ovary, and position 4 in oviduct in the 0.35 mg/kg dose group. Methylation decreases at position 3 and 5 in oviduct at dose 0.35 mg/kg, and decreases at position 5 and 6 in the 0.15 mg/kg dose group in uterus. Single stars indicate p-values<0.05, double stars indicate p-values<0.005, when compared to controls. Error bars indicate standard error.